Electronic properties of single-crystal α-Al_2O_3 films on Ru(0001)

2003 J. Phys.: Condens. Matter 15 8165

(http://iopscience.iop.org/0953-8984/15/47/019)

INSTITUTE OF PHYSICS PUBLISHING JOURNAL OF PHYSICS: CONDENSED MATTER

J. Phys.: Condens. Matter **15** (2003) 8165–8176 PII: S0953-8984(03)59992-1

Electronic properties of single-crystal α-Al_2O_3 films on Ru(0001)

Kazuo Nagata[1,3], **Chikashi Yamada**[1], **Toshio Takahashi**[2] **and Yoshitada Murata**[1]

[1] Physics Department, University of Electro-Communications, 1-5-1 Chofugaoka, Chofu, Tokyo 182-8585, Japan
[2] Institute for Solid State Physics, University of Tokyo, 5-1-5 Kashiwanoha, Kashiwa, Chiba 277-8581, Japan

E-mail: nagata@phys.uec.ac.jp

Received 13 February 2003
Published 14 November 2003
Online at stacks.iop.org/JPhysCM/15/8165

Abstract

A single-crystal film of α-Al_2O_3 was grown on the Ru(0001) surface with thicknesses of 6.5, 12 and 30 Å and a overlayer plasmon was found for 6.5 and 12 Å thick films. The dispersion relation as a function of wavevector parallel to the surface $q_{\|}$ was observed to have a negative gradient in the $\bar{\Gamma}$–$\bar{M}$ direction using angle-resolved electron-energy-loss spectroscopy (AREELS). This relation is as expected for the overlayer plasmon due to the collective motion of electrons in the oxide layer along the direction perpendicular to the surface. The energy of the overlayer plasmon is closely related to the interband transition energy: the latter plus depolarization shift equals the former. From the energy loss at the $\bar{\Gamma}$ point and the dispersion relation we arrived at the conclusion that intrinsic bandgap narrowing occurred. AREELS measurements with $\tau = 12$ and 30 Å support that the overlayer plasmon leading to the bandgap narrowing is caused by a strong interaction of the excited electron and hole inside the thin film with the image dipole induced in the metal substrate.

1. Introduction

When a thin single-crystal layer of oxide is fabricated on metal with high quality, interesting physics for fundamental materials research with respect to their electronic properties will be developed. At the interface between insulator and metal, the conduction electron density changes by orders of magnitude over a very short distance. The image potential near the interface shows rapid variation depending on the screening length in the two materials. A well-ordered oxide film on the metal surface is expected to have characteristic electronic properties

[3] Author to whom any correspondence should be addressed.

originating from the contact of two different materials. Inkson [1–4] showed theoretically that the band structure will be distorted in the interface region of the metal–semiconductor system due to a plasmon with a lower energy than the direct bandgap. The low-energy plasmon is affected strongly by the image potential. Anderson and Inkson claimed that the effective bandgap of covalent semiconductors becomes narrower in the vicinity of the metal due to a low-energy plasmon generated by many-body effects [5, 6]. Subsequently, Okiji *et al* [7] performed theoretical calculations and concluded that the insulator–metal transition in the insulator is caused by many-body effects at the interface, when the energy gap of the insulator is as small as 1 eV. A similar conclusion of bandgap narrowing due to many-body effects was obtained for an Al/GaAs(110) interface using first-principles calculations by Charlesworth *et al* [8].

In the case of an oxide with a wide bandgap, the electron density change at the interface is more drastic. The band structure in a thin single-crystal oxide layer is affected strongly by conduction electrons of the substrate metal through many-body effects, i.e. the interaction between excited electron and hole in the oxide and an image dipole in the metal. However, an understanding of the electronic properties of thin single-crystal oxide layers on metals is still limited and experimental studies have scarcely been performed except for electronic structure changes in the bandgap based on the surface defect and dislocation. Recently, thin single-crystal oxide films with high quality have been fabricated for α-Al_2O_3 on Ru(0001) by Murata *et al* [9] and β-SiO_2 on Ni(111) by Kundu and Murata [10], offering good candidates for studying the electronic properties.

In a previous paper [9], electron-energy-loss spectroscopy (EELS) and scanning tunnelling spectroscopy were used to study the bandgap of α-Al_2O_3 films on Ru(0001). An unexpected tendency was found in that the bandgap becomes narrower as the thickness decreases. In the present paper, we have measured a dispersion relation of the overlayer plasmon in α-Al_2O_3 films on Ru(0001), 6.5, 12 and 30 Å thick, using angle-resolved electron-energy-loss spectroscopy (AREELS). The interband transition energy has been estimated to be 5.6 eV from the plasmon dispersion relation in the overlayer 6.5 Å thick and the bandgap is approximated by 4.4 ± 0.5 eV from the onset of the overlayer plasmon excitation. The α-Al_2O_3 crystal has a wide bandgap and is characterized by mixed covalent and ionic bonding [11], so that it is basically a different material from that in the above-mentioned theoretical works on bandgap narrowing phenomena.

AREELS using low-energy electrons for the surface and interface plasmon excitations is one of the powerful tools to study surfaces and thin films. For example, an initial oxidation process of aluminium was studied by surface plasmons of Al by Murata and Ohtani [12]. There are many experimental studies of surface plasmon dispersion, which were reviewed by Rocca [13], and the theoretical works are listed in his review. On the other hand, there are only a few works on the overlayer plasmon. Theoretical work was performed by Newns using a simple model of a metallic layer one atom thick [14]. K chains on Si(001) were experimentally studied by Aruga *et al* [15]. With reference to this experimental work, several theoretical works were carried out by Ishida and Tsukada [16–18] and Nakayama *et al* [19].

2. Experimental details

The single-crystal α-Al_2O_3 film was grown on a Ru(0001) surface in an ultra-high vacuum (UHV) chamber equipped with a low-energy electron diffraction (LEED) optics and an AREEL spectrometer. The Ru(0001) surface, which is a refractory metal with a high melting point and which has an excellent lattice match with α-Al_2O_3(0001), was chosen as the metal substrate. The Ru(0001) surface was cleaned by repeated cycles of heating at 950 °C in an oxygen ambient

(3×10^{-5} Pa) followed by UHV annealing to 1200 °C. The Ru(0001) surface cleanliness was confirmed by LEED, where a clear six-fold symmetry was observed, and by Auger electron spectroscopy (AES), where no contamination species were detected.

Subsequently, aluminium ~10 Å thick was deposited on the Ru surface at 100 °C by thermal evaporation from a tungsten basket and then completely oxidized in an oxygen ambient of 2.0×10^{-4} Pa with gradually increasing temperature up to 1050 °C, to allow a phase transition from γ-Al_2O_3 to α-Al_2O_3 to occur. The thickness of the α-Al_2O_3 film was 6.5 Å and formation of α-Al_2O_3 was confirmed by observing a clear 1×1 LEED pattern [9]. Since the electron coherent length of the present LEED system is only 100 Å, we were not able to judge the large-scale surface quality by LEED. Therefore, the surface of the single-crystal film was observed by a scanning tunnelling microscope (RHK Technology, UHV 300). The single-crystal α-Al_2O_3 film was found to have a single domain of defect-free surface over a region of $0.5 \times 0.5\ \mu m^2$. The thickness τ of the α-Al_2O_3 film was estimated from an Auger electron signal and $\tau = 6.5$ Å corresponds to half the unit cell length along the c axis. Thicker oxide films were obtained by repeating the same process of Al deposition and oxidation several times. In the present experiment, we prepared three different samples of oxide thicknesses of 6.5, 12 and 30 Å.

The crystallinity of the α-Al_2O_3 film along the direction of the surface normal was examined by x-ray diffraction using synchrotron radiation at the beam line BL-9C of the Photon Factory, KEK. A separately prepared sample of thickness 15 Å was used. The beam line is equipped with a four-circle diffractometer and x-ray diffraction was measured using monochromatized x-rays of wavelength 1.0 Å. The intensity profile of the 00 rod was observed simply by θ–2θ scan (L scan) measurement for the α-Al_2O_3 film on Ru(0001) at $\tau = 15$ Å. In addition to the allowed reflections at $L = 2$ and 4, very sharp peaks at $L = 1$ and 3 were also observed, although these reflections are forbidden for Ru(0001) by the extinction rule. Then, the 00 rod profile was measured precisely, in which each data point was the integrated intensity of the profile obtained by ω-scan measurement, around $L = 1$, as shown in figure 1. The full width at half-maximum ΔL is less than 0.1. Although the $L = 1$ reflection was also found in the Ru(0001) surface covered with a natural oxide film, the integrated intensity of this peak from the Ru(0001) surface is only 1% of that from the α-Al_2O_3 film ($\tau = 15$ Å) on Ru(0001). The results show clear evidence for three-dimensional crystallization of the α-Al_2O_3 film on Ru(0001). The width ΔL for the peak for $L = 1$ is related to the thickness τ of the α-Al_2O_3 film by the kinematical expression $\tau \sim c_{Ru}/\Delta L$, where c_{Ru} is the lattice constant of the Ru c axis. Thus, τ is estimated to be ~40 Å, somewhat larger than the 15Å estimated previously. The origin of this discrepancy is not clear at present.

The EEL spectra were recorded with the AREEL spectrometer which consists of a 127° deflector-type electron monochromator and a hemispherical deflector-type analyser with a decelerating lens system, which was operated as a zoom lens for the present experiment. The angular and energy resolutions were 0.5° and $\leqslant$0.2 eV, respectively. The monochromator is fixed in position, whereas the analyser and the sample can be rotated independently around the common vertical axis. This allows independent variation of the incidence angle θ_i and emission angle θ_e, where both angles are measured from the surface normal.

When EEL spectra are observed as a function of θ_e with a fixed primary electron energy E_p and with a fixed θ_i, the dispersion relation for the surface excitation is deduced. From the energy and the momentum conservation in the specular reflection for inelastic scattering, as depicted in figure 2, a momentum transfer parallel to the surface $q_\parallel$ is determined as

$$q_\parallel = \frac{\sqrt{2mE_p}}{\hbar}\left(\sin\theta_i - \sqrt{1 - \frac{\Delta E}{E_p}}\sin\theta_e\right), \tag{1}$$

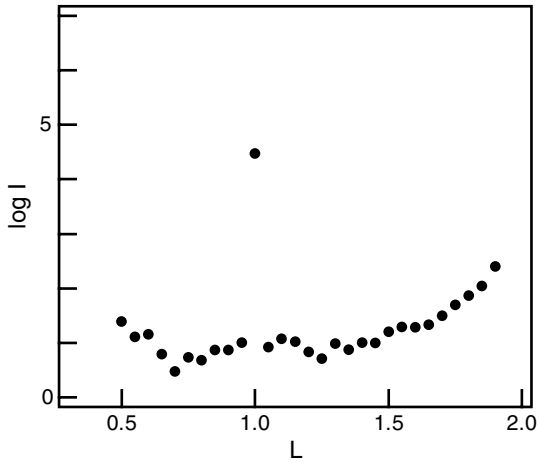

Figure 1. The 00 rod profile of x-ray diffraction from 15 Å thick α-Al_2O_3 film on Ru(0001) at $\tau = 15$ Å.

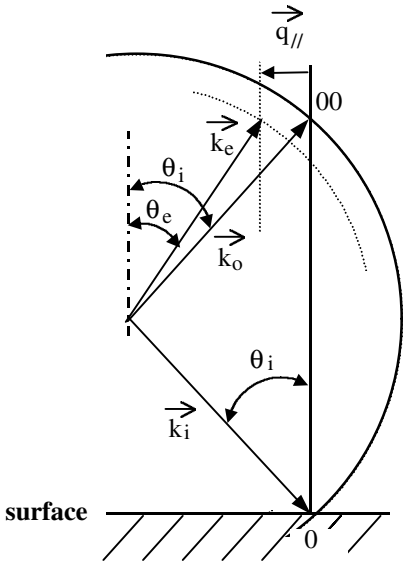

Figure 2. Scattering geometry of AREELS for measuring the dispersion relation on the basis of the Ewald construction.

where m is the electron mass and ΔE is the energy loss. The values of E_p and θ_i are usually fixed at a peak position of the I–V curve of the 00 rod. In the measurements, the quality of the crystal of the overlayer and surface flatness are very important. If there exists an imperfect area and/or a rough surface region, elastically scattered electrons would give an undesirable background in the direction of θ_e. As a consequence, a wrong flat dispersion in the dispersion relation would be found. The crystal azimuth was aligned in the direction of $\bar{\Gamma}$–$\bar{M}$ and the angle of incidence and the electron energy was set to the maximum intensity corresponding to the 004 Bragg reflection from the Ru(0001) substrate.

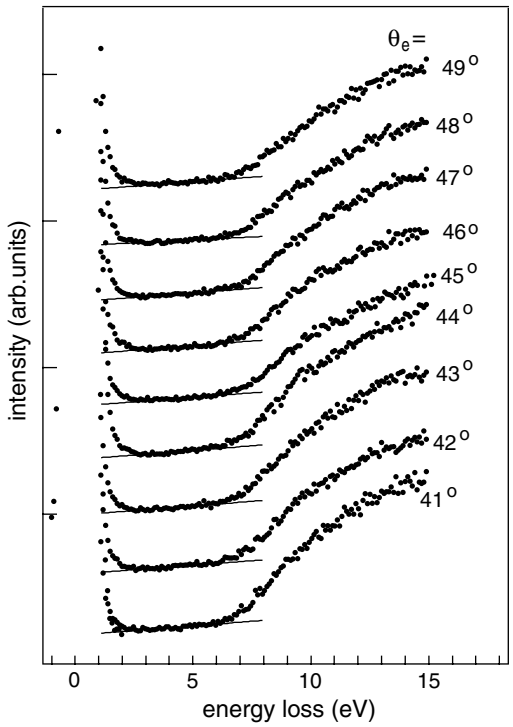

Figure 3. AREEL spectra of a 30 Å-thick α-Al_2O_3 film on Ru(0001) as a function of θ_e in the $\bar{\Gamma}$–$\bar{M}$ direction. $E_p = 60$ eV, $\theta_i = 45°$.

3. Results

Figure 3 shows AREEL spectra as a function of emission angle θ_e measured from the 30 Å-thick α-Al_2O_3 film. All of the spectra have a common onset, which is found at 6.4 ± 0.2 eV. This value of 6.4 eV is in good agreement with the onset in the imaginary part of the complex refractive index 6.8 eV obtained from optical measurements by Arakawa and Williams on amorphous Al_2O_3 films with thicknesses of 200–1000 Å [20]. The absorption edge observed in the optical measurement is shifted to a lower energy of 6.8 eV by the exciton excitation, which is peaked at 8.4 eV, from the band-to-band transition edge at 9.4 ± 0.4 eV. Similarly, the onset in figure 3 is given by the exciton absorption edge, although a clear exciton excitation peak cannot be observed. The exciton peak may have disappeared due to the small number of excitons in a thin layer. Therefore, 30 Å-thick α-Al_2O_3 film is considered to take a band structure similar to the bulk one.

A remarkable difference was observed in a thin α-Al_2O_3 film on Ru(0001) with $\tau = 6.5$ Å. Figure 4 shows AREEL spectra as a function of θ_e measured from the 6.5 Å-thick α-Al_2O_3 film. The common onset is 4.4 ± 0.2 eV, showing bandgap narrowing, compared with that of thicker films, 6.4 eV. Each of the spectra has two peaks around 7 and 11 eV. Indicating clearly the two energy loss peaks, difference spectra are shown in figure 5 by subtracting numerically the corresponding spectrum with the same or near θ_e shown in figure 3 from each spectrum of figure 4. Each first energy loss peak in the difference spectra was fitted to a Gaussian shape as shown by a full curve and the peak position is indicated by an arrow. The fact that this peak is represented by a symmetric Gaussian shape indicates there are few excitons in such a thin oxide layer as $\tau = 6.5$ Å.

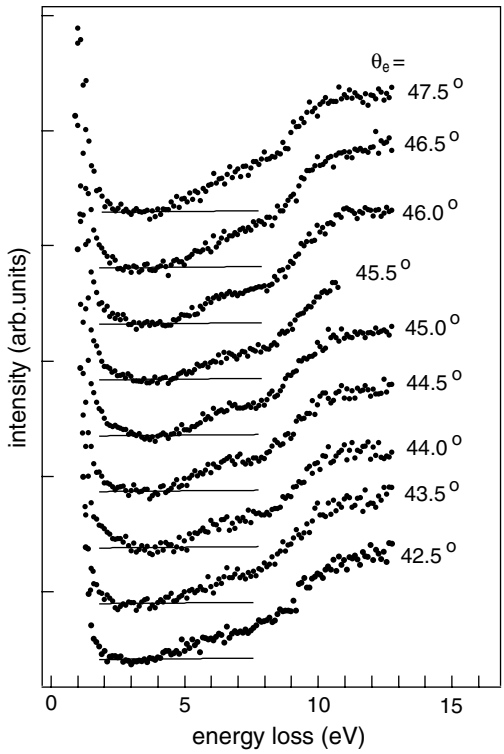

Figure 4. AREEL spectra of a 6.5 Å-thick α-Al_2O_3 film on Ru(0001) of various θ_e's in the $\bar{\Gamma}$–$\bar{M}$ direction. $E_p = 65$ eV, $\theta_i = 44.5°$.

A significant consequence is that dispersion of the peak position was observed in the difference spectra as a function of θ_e. The dispersion relation as a function of $q_\parallel$ was calculated using equation (1) where $\theta_e = 47.9°$ at $q_\parallel = 0$. A linear dispersion starting from $\Delta E = 6.6$ eV with a negative gradient was obtained as shown in figure 6.

This energy loss is considered to be due to the excitation of an overlayer plasmon originating from the interband (valence- to conduction-band) transition [19]. The negative dispersion in an overlayer plasmon can be explained by charge fluctuation polarized perpendicular to the overlayer and by the depolarization shift. All the dipoles oscillate in phase at the $\bar{\Gamma}$ point, as shown by full arrows in figure 7(a) and the adjacent polarization field enhances the transition energy corresponding to the plasmon excitation. Thus, the $\bar{\Gamma}$ point has the largest plasmon energy, which is the sum of the interband transition energy and the depolarization shift [17]. Since the content of the out-of-phase dipole oscillation increases with increasing $q_\parallel$, the depolarization field is partially cancelled by adjacent dipoles. Finally, the largest depolarization shift in the negative direction is obtained at the Brillouin zone boundary, i.e. at the $\bar{M}$ point in the present case (figure 7(b)). The linear dispersion relation with a negative gradient is expected.

This scheme shows that the largest depolarization shift in the positive direction appears at $q_\parallel = 0$. That is, the overlayer plasmon energy at $\bar{\Gamma}$ of 6.6 eV is higher than the interband transition energy of the oxide layer by the depolarization shift. The data points in the dispersion relation are fitted by a linear function indicated by a broken line in figure 6. The position of $q_\parallel = 0.25$ Å^{-1} is near to the middle point of the $\bar{\Gamma}$–$\bar{M}$ vector, since the $\bar{M}$ point is located

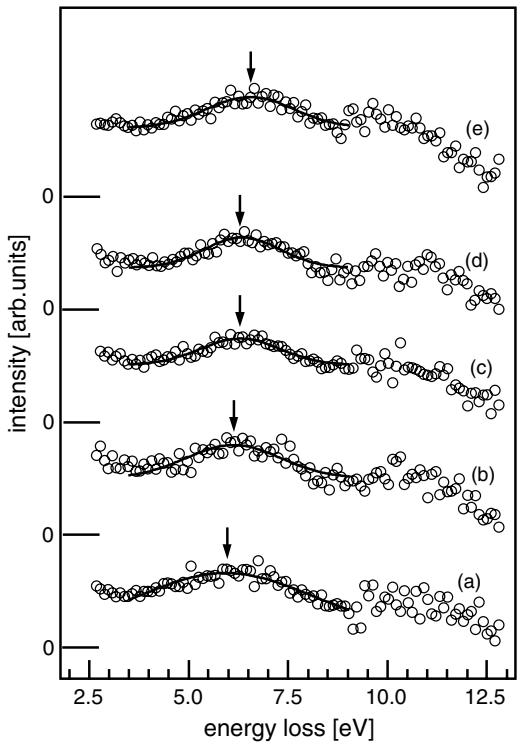

Figure 5. Difference spectra of the 6.5 Å-thick α-Al_2O_3 film after subtraction of the corresponding spectra of the 30 Å-thick α-Al_2O_3 film. The full curve shows the fitted Gaussian curve and the maximum position is indicated by the arrow. (a) $\theta_e = 42.5°$ ($\tau = 6.5$ Å)-$\theta_e = 43°$ ($\tau = 30$ Å), (b) 44°-44°, (c) 45°-45°, (d) 46°-46° and (e) 47.5°-48°.

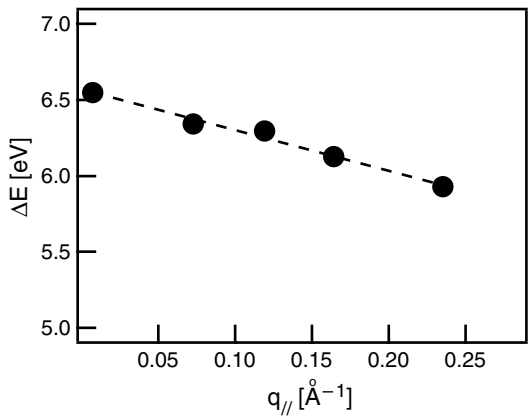

Figure 6. Dispersion relation of the overlayer plasmon in the $\bar{\Gamma}$–$\bar{M}$ direction. Data are fitted by a linear function of the broken line.

at $q_\parallel = 0.66$ Å^{-1}. If the linear relation is satisfied in the whole range of $\bar{\Gamma}$–$\bar{M}$, the plasmon energy at $\bar{M}$ is extrapolated to be 4.6 eV. Thus, the interband transition energy E_t is given by 5.6 eV, provided that the absolute value of the depolarization shift at $\bar{M}$ is assumed to be

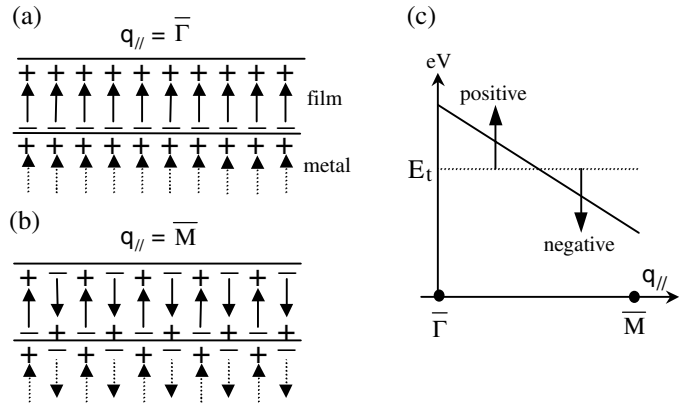

Figure 7. Schematic representation of the dipole distribution in the oxide layer and image dipoles (a) at $q_{\parallel} = 0$ ($\bar{\Gamma}$ point) and (b) at the $\bar{M}$ point. (c) Depolarization shift of the overlayer plasmon as a function of $q_{\parallel}$.

equal to that at $\bar{\Gamma}$ (figure 7(c)). This value shows that the bandgap narrowing occurs in the 6.5 Å-thick α-Al_2O_3 film on Ru(0001) and the bandgap is approximated from the onset of the AREEL spectra, 4.4 ± 0.5 eV, in which the error limit has been re-estimated because the onset of the plasmon excitation varies with observation angle. This reduction of the bandgap is due to a strong interaction of the excited electron and hole in the thin oxide layer with the image dipole in the substrate metal.

4. Discussion

The microscopic theory of such a collective excitation inside the thin overlayer was initiated by Newns [14], though the effect of the substrate is not considered. An alkali-metal overlayer was described by free electrons confined between infinite potential barriers for a uniform thin film as a particle-in-a-box model. This model predicts the negative linear dispersion in a small $q_{\parallel}$ region (B mode). A more adaptable model was developed by Ishida *et al* [17] as a realistic picture for overlayer plasmons. A parallel-rod model was employed to explain the K overlayer plasmon on Si(001) 2×1-K [15]. A physical scheme of the positive and negative dispersion of the overlayer plasmon in a small $q_{\parallel}$ region has been described and the negative dispersion corresponds to the s–p_z interband mode.

It is necessary to clarify that the observed peak assigned to the overlayer plasmon did not originate from defects, impurities or some sort of interface states. The energy loss from the localized state, such as an impurity level, has a flat dispersion, whereas the dispersion shown in figure 6 has a negative slope. In addition, any chemical shifts of the Ru Auger electron signal due to oxidation of the Ru metal was not observed in AES spectra, thereby indicating that no Ru oxide phase exists in the interface region. Confirming that the observed energy loss peak did not originate from states such as the undesirable poor quality of the oxide film or oxide/metal interface but was from the overlayer plasmon, AREEL spectra as a function of θ_e were observed for the α-Al_2O_3 film on Ru(0001) with $\tau = 12$ Å (nearly the same length as the electron mean free path). In this case, no energy loss peak around 6 eV was found in any emission angle, as shown in figure 8(a).

Here we discuss the second peak in the difference spectrum of figure 5. Because the film thickness is shorter than the electron mean free path, it is possible to detect the energy loss

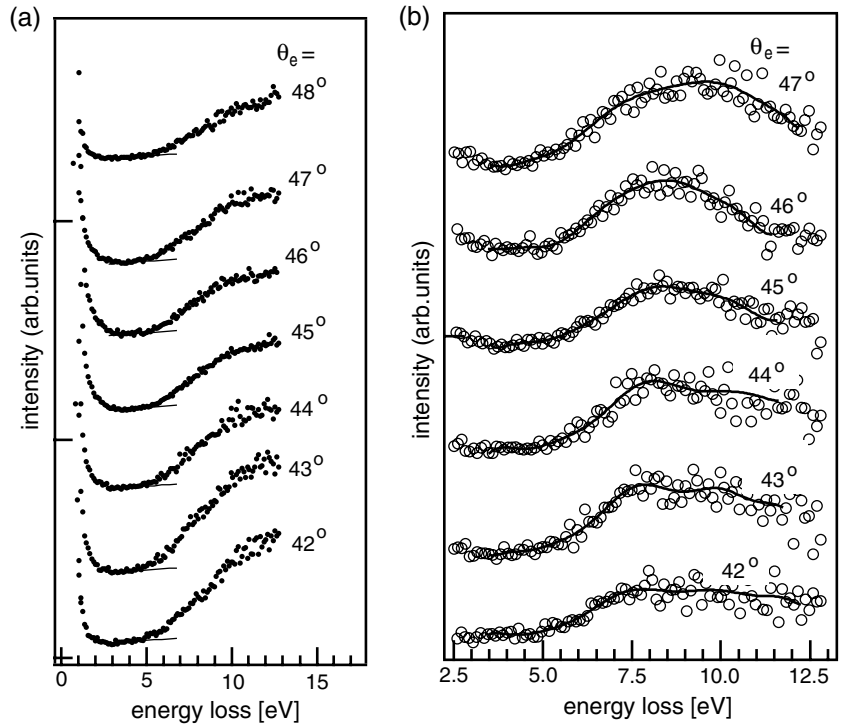

Figure 8. (a) AREEL spectra of the 12 Å-thick α-Al_2O_3 film on Ru(0001) as a function of θ_e in the $\bar{\Gamma}$–$\bar{M}$ direction. $E_p = 65$ eV, $\theta_i = 45°$. (b) Difference spectra of the film after subtraction of the corresponding spectrum of the 30 Å-thick α-Al_2O_3 film. The full curve is a guide to the eye.

spectrum of the metal substrate. Figure 9 shows an EEL spectrum of a clean Ru(0001) surface. A prominent plasmon loss peak is found at 10.2 eV together with the two- and three-plasmon loss peaks (at 22 and 32 eV, respectively). This energy loss peak is assigned to the volume plasmon of Ru, since the volume plasmons of transition metals have similar energies [21]. Therefore the second peak appearing at 10–11 eV in the difference spectra of 6.5 Å-thick α-Al_2O_3 film is assigned to the volume plasmon of the Ru substrate (possibly containing a contribution from two-overlayer plasmon loss).

Since the bulk plasmon of the Ru substrate is observed through the 6.5 Å-thick oxide film, it is feared that the first peak might originate from the surface plasmon of Ru(0001) covered with the oxide layer. This concern is eliminated by the result of the difference spectra for the 12 Å-thick oxide layer. Figure 8(b) shows the difference spectra obtained by subtracting the corresponding spectrum of the 30 Å-thick oxide film from each spectrum of figure 8(a). The full curve is fitted by a polynomial as a guide to the eye. There seems to be two peaks, one at ∼8 eV and the other at ∼10 eV. The latter corresponds to the bulk plasmon loss of the Ru substrate. It is noted that the first peak (∼8 eV) is higher in energy than that (∼6 eV) of a 6.5 Å thick sample. When a free-electron metal is covered with an oxide layer of thickness τ, the dispersion relation of the surface plasmon of the metal is given by

$$\hbar\omega_s = \hbar\omega_p \left[\frac{\varepsilon + \tanh q_\parallel \tau}{2\varepsilon + (1+\varepsilon^2)\tanh q_\parallel \tau} \right]^{1/2}, \tag{2}$$

where $\hbar\omega_p$ is the volume plasmon energy and ε is the dielectric constant of the oxide overlayer [22]. According to equation (2), the surface plasmon energy $\hbar\omega_s$ decreases

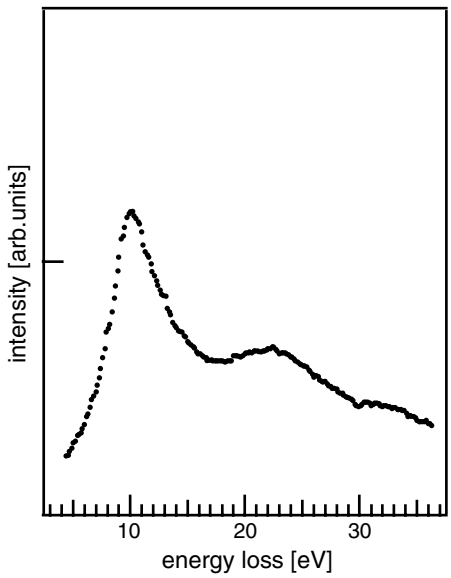

Figure 9. EEL spectrum from the clean Ru(0001) surface. $E_p = 60$ eV and $\theta_i = \theta_e = 45°$.

monotonically with increasing oxide thickness from $\hbar\omega_s = \hbar\omega_p/\sqrt{2}$ at $\tau = 0$ to $\hbar\omega_p/\sqrt{1+\varepsilon}$ at $\tau = \infty$. This tendency is satisfied in the surface plasmon of the transition metal. In contrast, the present result shows that the energy loss of the first peak increases with increasing oxide thickness. Therefore, the energy loss appearing at ~6 eV in the difference spectrum of the 6.5 Å-thick oxide layer (figure 5) is not the surface plasmon loss due to the Ru(0001) induced by the oxide layer. Thus, the dispersion relation observed in the 6.5 Å-thick α-Al_2O_3 film on Ru(0001) (figure 6) is that of the overlayer plasmon.

The increase in the overlayer plasmon energy with oxide thickness is due to the fact that the interaction of the excited electron and hole in the oxide layer with the image dipole in the metal becomes weaker with increasing oxide thickness. This view is supported by observing the volume plasmon of the α-Al_2O_3 film. Figure 10 shows EEL spectra of α-Al_2O_3 films of $\tau = 6.5$, 12 and 30 Å over a wider energy range (0–27 eV). The energy loss peaks appear at ~21 eV in $\tau = 12$ and 30 Å samples. This energy loss peak corresponds to the energy of the Al_2O_3 volume plasmon [23], whereas the loss peak at ~21 eV is absent in the $\tau = 6.5$ Å sample. Thus, the overlayer plasmon is excited in the case of $\tau = 6.5$ Å instead of the volume plasmon. The strong interaction of the charge fluctuation in the oxide layer with the image dipole in the substrate metal is significant in the thin oxide layer and the volume plasmon is converted to the overlayer plasmon. In the case of $\tau = 12$ Å, both the overlayer plasmon and the volume plasmon are observed because of a weak interaction.

The bandgaps, determined by the onset of the energy loss spectrum, are 4.4 ± 0.2, 5.1 ± 0.3 and 6.4 ± 0.2 eV for thickness of 6.5, 12 and 30 Å (see also figure 8(a)). Thus, the bandgap increases with film thickness, or the bandgap narrowing occurs towards the thinner oxides. It should be noted that the bandgap narrowing is due to many-body effects in two respects. First, the overlayer plasmon appears through many-body effects. Second, the strong coupling, which reduces the bandgap, between the electron and hole excited in the thin film and the image dipole induced in the substrate is also a many-body effect.

Inkson and Anderson proposed that the bandgap in a semiconductor or an insulator decreases due to the presence of low-energy plasmons near the interface due to the charge

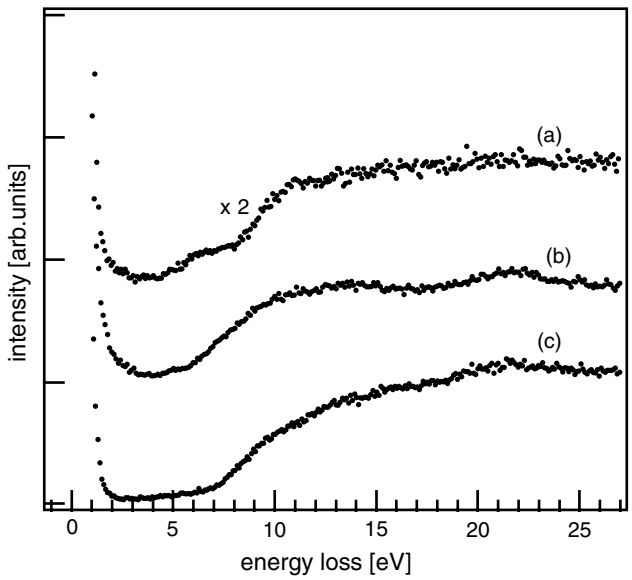

Figure 10. EEL spectra over a wider energy loss range (0–27 eV) for various thicknesses of α-Al_2O_3 films; (a) $\tau = 6.5$ Å, $E_p = 65$ eV, $\theta_i = 44.5°$ and $\theta_e = 46°$, (b) $\tau = 12$ Å, $E_p = 65$ eV, $\theta_i = \theta_e = 45°$, (c) $\tau = 30$ Å, $E_p = 60$ eV, $\theta_i = \theta_e = 45°$.

fluctuations coupled with the image potential, and interpreted the bandgap narrowing by many-body effects at the interfaces [5]. In the present result, we have showed that the overlayer plasmon in the bulk bandgap exists and the overlayer plasmon induces the bandgap narrowing. However, the depth dependence of the bandgap narrowing is quite different from that of the Inkson–Anderson model, where the low-energy plasmon appears around the interface, independent of the insulator thickness. In the present case, on the other hand, the overlayer plasmon has a constant energy over the whole region of the oxide layer. Consequently, the bandgap narrowing occurs equivalently through the thin oxide layer, i.e. no depth dependence of bandgap narrowing, whereas the narrowing could not be found at the interface for the thicker oxide layer, in contrast with the Inkson–Anderson model.

The bandgap narrowing in the oxide layer on the metal has been found in the single-crystal α-Al_2O_3 film on Ru(0001). A longer lifetime of the excited electron and hole is expected in the single-crystal oxide than in amorphous or polycrystalline oxides. Thus, we were able to observe the intrinsic bandgap narrowing in a high-quality single-crystal film such as the present system with $\tau = 6.5$ Å. On the other hand, Coshina and Franchy [24] investigated the bandgap of amorphous and γ-Al_2O_3 formed on $Ni_3Al(100)$. The lowering of the bandgap with respect to the bulk value was concluded to be associated with the defect-induced state in the bandgap, in contrast to the present study.

5. Conclusion

High quality single-crystal films of α-Al_2O_3 have been grown on Ru(0001) surfaces. The plasmon dispersion against $q_\parallel$ was observed as a negative linear relation in the 6.5 Å-thick α-Al_2O_3 film and was recognized as an overlayer plasmon caused by the charge fluctuation relevant to the interband transition in the oxide film. We arrived at the conclusion that

intrinsic bandgap narrowing occurred, where the interband transition energy was estimated to be 5.6 eV from the plasmon dispersion relation. The narrowed bandgap was approximated by 4.4 ± 0.5 eV from the onset of the AREEL spectrum. AREELS measurements with $\tau = 12$ and 30 Å support the idea that the overlayer plasmon leading to bandgap narrowing is caused by a strong interaction of the excited electron and hole inside the thin film with the image dipole induced in the metal substrate.

Acknowledgments

This work was supported by a Grant-in-Aid for Scientific Research (B) from Ministry of Education, Culture, Sports, Science and Technology. Synchrotron x-ray diffraction experiments were performed under the approval of the Photon Factory (PF-PAC nos 2000S2003 and 2001G055).

References

[1] Inkson J C 1971 *Surf. Sci.* **28** 69
[2] Inkson J C 1971 *J. Phys. C: Solid State Phys.* **4** 591
[3] Inkson J C 1972 *J. Phys. C: Solid State Phys.* **5** 2599
[4] Inkson J C 1973 *J. Phys. C: Solid State Phys.* **6** 1350
[5] Anderson P W 1974 *Elementary Excitations in Solids, Molecules and Atoms,* part A (New York: Plenum) p 1
[6] Inkson J C 1974 *J. Vac. Sci. Technol.* **11** 943
[7] Okiji A, Kasai H and Terakawa S 1978 *J. Phys. Soc. Japan* **44** 1275
[8] Charlesworth J P A, Gogby R W and Needs R J 1993 *Phys. Rev. Lett.* **70** 1685
[9] Murata Y, Nagata K, Fujimoto H, Sakurai T, Okada M and Ebe Y 2001 *J. Phys. Soc. Japan* **70** 793
[10] Kundu M and Murata Y 2001 *Appl. Phys. Lett.* **80** 1921
[11] French R H 1990 *J. Am. Ceram. Soc.* **73** 477
[12] Murata Y and Ohtani S 1972 *J. Vac. Sci. Technol.* **9** 789
[13] Rocca M 1995 *Surf. Sci. Rep.* **22** 1
[14] Newns D M 1972 *Phys. Lett.* A **38** 341
[15] Aruga T, Tochihara H and Murata Y 1984 *Phys. Rev. Lett.* **53** 372
[16] Tsukada M, Ishida H and Shima N 1984 *Phys. Rev. Lett.* **53** 376
[17] Ishida H, Shima N and Tsukada M 1985 *Phys. Rev.* B **32** 6246
[18] Ishida H and Tsukada M 1986 *Surf. Sci.* **169** 225
[19] Nakayama M, Kato T and Ohtomi K 1984 *Solid State Commun.* **50** 409
[20] Arakawa E T and Williams M W 1968 *J. Phys. Chem. Solids* **29** 735
[21] Raether H 1980 *Excitation of Plasmons and Interband Transitions by Electrons* (Berlin: Springer) p 54 (references are therein, though there are no data on Ru)
[22] Stern E A and Ferrell R A 1960 *Phys. Rev.* **120** 130
[23] Leder L B 1956 *Phys. Rev.* **103** 1721
[24] Costina I and Franchy R 2001 *Appl. Phys. Lett.* **78** 4139